MYCOBIOLOGY
2026, VOL. 0, NO. 0, 1–19
https://doi.org/10.1080/12298093.2026.2675762

RESEARCH ARTICLE

OPEN ACCESS Check for updates

Whole Genome Sequence of *Xylaria chamelensis* (Xylariales, Ascomycota), A New Species Associated with Fabaceae Pods

Yulena Osorio-Navarro[a,b], Ricardo Valenzuela[a], César Hernández-Rodríguez[b], Tania Raymundo[a], Abigail Pérez-Valdespino[c], Hannya Chamorro-Martínez[a,b] and Juan Alfredo Hernández-García[b]

[a]Departamento de Botánica, Instituto Politécnico Nacional, Escuela Nacional de Ciencias Biológicas, Laboratorio de Micología, Mexico City, Mexico; [b]Departamento de Microbiología, Instituto Politécnico Nacional, Escuela Nacional de Ciencias Biológicas, Laboratorio de Biología Molecular de Bacterias y Levaduras, Mexico City, Mexico; [c]Departamento de Bioquímica, Instituto Politécnico Nacional, Escuela Nacional de Ciencias Biológicas, Laboratorio de Ingeniería Genética, Mexico City, Mexico

ABSTRACT

The cosmopolitan genus *Xylaria* Hill ex Schrank (Ascomycota, Sordariomycetes), is the largest within the order Xylariales. While *Xylaria* species primarily exist as saprotrophs, they can also occur as endophytes or as phytopathogens. Specimens of *Xylaria* sp. were collected from a Fabaceae pod in the tropical dry forest in the state of Jalisco, Mexico. They were isolated and axenized in PDA culture medium. The genome of the strain was sequenced using Illumina NovaSeq technology and assembled. A phylogenomic approach was used to confirm its taxonomic position within the genus *Xylaria*. The resulting genome assembly is 51.93 Mb in size, featuring an N50 of 452,556 bp and a G+C content of 42.34%. Gene prediction with AUGUSTUS identified 11,238 protein-coding genes. Based on morphological and genomic evidence, these specimens are described here as a new species, *Xylaria chamelensis* sp. nov. Phylogenomic analysis incorporating available *Xylaria* genomes revealed that this strain forms a distinct, independent lineage within the *Xylaria* phylogenetic tree. Ultimately, these genomic data provide the scientific community with a valuable resource to advance genome-based taxonomy, unravel the molecular basis of plant-fungus associations, and further explore the diverse metabolism of the genus *Xylaria* across tropical and subtropical environments.

ARTICLE HISTORY
Received 18 December 2025
Revised 7 May 2026
Accepted 11 May 2026

KEYWORDS
Genomics; fungi; Xylariaceae; phylogenomics; fungal taxonomy

1. Introduction

Xylaria is the largest genus within the order Xylariales (Ascomycota) with 602 accepted species in Index Fungorum (http://www.indexfungorum.org/Names/Names.asp, accession date: September 30, 2025). This genus is morphologically defined by perithecia embedded in dark stromata, asci with an amyloidal apical pore, and unicellular ascospores with a germ slit. It is distributed worldwide but is highly diverse in the tropics and subtropics [1]. *Xylaria* species can be found on lignocellulosic substrates such as dead wood and branches. In contrast, some species are associated with fallen leaves and petioles, fallen fruits, seeds, and termite nests [2], grouped into polyphyletic clades within the genus [3,4].

Species-level identification within the genus *Xylaria* remains difficult due to high morphological similarity among taxa and numerous species complexes; however, integrative taxonomic approaches have proven effective in revealing new data, including the description of new species and the clarification of phylogenetic relationships within the genus [2,3]. Recent studies of *Xylaria* genomic data helped establish relationships among major clades within the genus, as well as their metabolites of interest [5]. Furthermore, fungal genomes in the order Xylariales are known to possess some of the highest numbers of genes associated with secondary metabolism among all fungi [6,7]. Consequently, the main objective of this study is to obtain the genome sequence from a new *Xylaria* species isolated from a Fabaceae pod in Mexico.

2. Materials and methods

2.1. Morphological characterization and isolation of Xylaria sp. strain RV14508

A review of *Xylaria* specimens deposited in the ENCB herbarium revealed a fungus collected growing on a Fabaceae pod in a tropical dry forest at the Chamela

CONTACT Juan Alfredo Hernández-García freddyhardcore@gmail.com
Supplemental data for this article can be accessed online at https://doi.org/10.1080/12298093.2026.2675762.

Biological Station of the Instituto de Biología, Universidad Nacional Autonóma de México, in the State of Jalisco, Mexico. This specimen was identified as a *Xylaria* sp. that is not conspecific with other *Xylaria* species known to grow on pods, such as *Xylaria ianthinovelutina* (Mont.) Fr. and *Xylaria oxyacanthae* Tul & C. Tul., both belonging to distinct clades within *Xylaria sensu lato* (s.l.). Moreover, the latter has recently been transferred to the genus *Heteroxylaria* as *Heteroxylaria oxyacanthae* (Tul. & C. Tul.) Hai X. Ma, A.H. Zhu & Y. Li [8]. Hence, the specimen tagged as RV14508 was thereafter isolated, axenized on potato dextrose agar (PDA), and incubated for 7 d at 25 ± 2 °C (in the dark) to obtain high-molecular-weight genomic DNA. The strain RV14508 was designated as the ex-type, considering that it was deposited in a metabolically inactive state (at −70 °C in 30% glycerol) at the Escuela Nacional de Ciencias Biológicas del Instituto Politécnico Nacional (ENCB), Mexico City, Mexico, and successfully recovered in different culture media without losing viability or presenting changes in its colonial characteristics. Macroscopic characteristics of the ascomata and colony (mycelial color and surface texture) were recorded using a Nikon D5600 digital camera (Nikon, Tokyo, Japan). At the same time, microscopic features were assessed by examining preparations of 10 stromata under a light microscope (PrimoStar Optical, Carl Zeiss, Germany) to take at least 30 structural measurements for each structure, with the highest and lowest 5% of measurements excluded. Average size and Q values (length/width ratios) of ascospores are provided in parentheses. Structure colors were coded following the Munsell® Soil Color Chart [9].

2.2. DNA extraction and library preparation

Mycelial biomass from the isolated fungus was harvested, and 5 mm^2 was ground into a fine powder using a sterile mortar and pestle. DNA was extracted using a cetyltrimethylammonium bromide (CTAB)-based protocol [10]. DNA concentration and purity were determined using a Nanodrop 2000 spectrophotometer (Thermo Fisher Scientific, Waltham, MA). DNA integrity was assessed by agarose gel electrophoresis at 0.8%. To confirm the identity of *Xylaria* sp. strain RV14508, the internal transcribed spacer (ITS) and the nuclear large subunit ribosomal DNA (nrLSU) were amplified by PCR using universal primers ITS1 and ITS4 and the primer pair LR0R and LR7, respectively [11,12]. The resulting ITS and nLSU sequences were compared to the NCBI database using the BLASTn algorithm [13] and deposited in the GenBank database. Also, the sequences of β-tubulin and RPB2 genes were retrieved from the genomic annotation and are deposited in the same database.

The whole-genome library preparation and paired-end sequencing were performed at Novogene (Sacramento, CA), with a read length of 150 bp per end (PE150). Short reads were generated on the Illumina Novaseq platform (Illumina, San Diego, CA) using whole-genome shotgun libraries.

2.3. Genome assembly and annotation

The genome was first assembled *de novo* with SPAdes version 3.13.1 [14] using the – careful and –cov-cutoff auto options. The genome assembly quality was assessed using QUAST version 5.3.0 [15] based on scaffolds greater than 1000 bp. To improve the continuity of the *de novo* assembly, a reference-guided scaffolding strategy was implemented using RagTag version 2.1.0 [16]. The genome of *Xylaria scruposa* (Accession number: GCA_022385635.1) was selected as the reference sequence due to its phylogenetic proximity and the quality of the assembly. The workflow involved two main steps: first, the ragtag.py correct module was applied to identify and resolve potential chimeric contigs and misassemblies; second, the ragtag.py scaffold module was used to order and orient the corrected contigs into larger scaffolds. To minimize genomic noise and assembly artifacts, the resulting scaffolds were filtered to a minimum length of 1000 bp using SeqKit [17]. Assembly quality and continuity were assessed with QUAST version 5.3.0 [15], while genome completeness was evaluated against BUSCO (Benchmarking Universal Single-Copy Orthologs) version 6.0.0 [18] using the Xylariales lineage data set (xylariales_odb12).

Gene prediction was performed using AUGUSTUS version 3.5.0 [19], with *Neurospora crassa* Shear & B.O. Dodge as the training species (Ascomycota_odb10 dataset) and default settings. Gene annotation was performed using BLASTp [13] based on *Xylaria bambusicola* (accession number: GCA_022495145.1).

To gain insights into the metabolism of *Xylaria* sp. strain RV14508, biosynthetic gene clusters (BGCs) were predicted using antiSMASH version 8.0 [20] with the – taxon fungi option. The functional annotation of the predicted protein-coding genes was performed with the annotate module of the pipeline Funannotate version 1.8.17 (https://github.com/nextgenusfs/funannotate). Funannotate assigns genes to the prominent catalytic families described in the dbCAN2 version 2.0.11 [21], CAZymes databases [22,23]. These include carbohydrate-active enzymes (CAZymes) classified as follows: glycoside hydrolases (GHs), glycosyltransferases (GTs), polysaccharide lyases (PLs), carbohydrate-binding modules (CBMs),

Table 1. Details of the genome sequences used for phylogenomic analysis.

Species	Voucher	Accession number	Genome size (Mb)	Number of contigs	GC content (%)	Annotated genes	Remarks
Hypoxylon fragiforme	CBS 206.31	GCA_022984875.1	36.4	15	47	10,382	None
Xylaria acuta	CBS 122032	GCA_022495125.1	47.2	1,009	46.5	12,673	None
Xylaria arbuscula	CBS124340	GCA_022385695.1	51.2	141	44.5	13,122	RefSeq
Xylaria arbuscula	FL1030	GCA_022578905.1	52.1	1,391	44	12,934	RefSeq
Xylaria bambusicola	CBS 139988	GCF_022495145.1	45.7	377	45.5	12,324	RefSeq
Xylaria cf. *castorea*	CBS 124033	GCA_022495115.1	45.9	528	45.5	12,272	None
Xylaria chamelensis sp. nov. (This study)	RV14508	GCA_056151845	51.9	3,364	42.3	11,238	Locality: Jalisco, Mexico Host: Fabaceae pod
Xylaria cubensis	CBS 116.85	GCA_022385715.1	44.8	384	46	12,927	None
Xylaria curta	Babe10	GCA_027595895.1	44.2	5,810	48	10,891	None
Xylaria digitata	CBS 161.22	GCA_022495195.1	58.4	949	40	12,982	None
Xylaria feejeensis	Xyl2	GCA_051622775.1	50.6	1270	42	–	RefSeq Host: *Bambusa* sp.
Xylaria flabelliformis (*Xylaria curta*)	CBS 114988	GCA_022495235.1	43.9	319	47.5	13,249	None
Xylaria flabelliformis	G536	GCA_007182795.l1	41.2	162	47.5	11,404	Host: *Asimina triloba* (L.) Dunal
Xylaria grammica	IHI A82	GCA_004014815.1	47	1,058	48	12,126	Host: On deciduous woodland
Xylaria grammica	CBS 120713	GCA_022495055.1	50.8	973	46.5	13,411	Locality: Thailand
Xylaria hypoxylon	DSM 108379	GCA_004768795.1	42.8	637	47	11,038	Host: On deciduous woodland
Xylaria intraflava	YMJ 725	GCA_022385655.1	35.9	577	52	10,068	Locality: Taiwan
Xylaria longipes	CBS 148.73	GCA_025201785.1	50.8	1,054	42.5	12,755	None
Xylaria palmicola	CBS 124036	GCA_022385595.1	43.9	809	48	11,806	None
Xylaria polymorpha	DSM 105756	GCA_003426235.1	43.5	951	48.5	12,349	Host: *Fagus* L.
Xylaria scruposa	CBS 123580	GCA_022385635.1	46.6	625	45.5	13,297	None
Xylaria sp.	CBS 124048	GCA_022385685.1	33.7	853	50	9,104	None
Xylaria sp.	FL0043	GCA_022578865.1	44.5	974	46	11,979	Locality: Florida, USA
Xylaria sp.	FL0933	GCA_022578765.1	46.5	557	45	12,020	Locality: Florida, USA
Xylaria sp.	FL1042	GCA_022495085.1	57	2,637	39.5	12,257	Locality: Florida, USA
Xylaria sp.	FL1777	GCA_022578965.1	60.3	1,010	37.5	11,826	Locality: Florida, USA
Xylaria telfairii	CBS 121673	GCA_022495065.1	46.9	1,120	47	12,931	None
Xylaria venustula	FL0490	GCA_022578775.1	50.8	473	43	12,602	Locality: Florida, USA

carbohydrate esterases (CEs), and auxiliary activity enzymes (AAs). Protease characterization was performed by searching for homologies in the MEROPS version 12.4 database; annotated genes were grouped according to catalytic type (serine, aspartic, metallo, threonine, and cysteine proteases) and functional families (e.g., S09, A01, M28, etc.) [24].

2.4. Phylogenetic and phylogenomic analyses

The annotated genomes of fungal strains listed in Table 1 were used for comparative genome analyses. Orthogroups were identified using OrthoFinder version 2.5.4 [25], and the resulting protein alignments were used to infer a phylogenomic maximum-likelihood (ML) tree with IQ-TREE version 3.0.1 [26]. Protein evolutionary models were selected with ModelFinder [27] based on the corrected Akaike information criterion (AICc) and included in IQ-TREE. The analysis was conducted with 1000 ultrafast bootstrap (UFB) replicates combined with 1000 SH-aLRT replicates [28], employing the Q.mammal+F + R9 protein substitution model. A concatenated alignment of ITS, nLSU, RPB2, and β-tubulin sequences representative of the main clades within Table 2 was used to infer a multi-locus ML phylogeny in IQ-TREE version 3.0.1 [26]. The best evolutionary model for the alignment was also determined with ModelFinder [27] to assess branch support. 1000 nonparametric rapid bootstrap pseudo-replicates were run with the TN+R3 nucleotide substitution model using the Bayesian information criterion (BIC). Due to its taxonomic placement in the Hypoxylaceae (Xylariales), *Hypoxylon fragiforme* (Pers.) J. Kickx f. was selected as the outgroup for both analyses. The trees were visualized in Figtree version 1.4.4 [29] and further edited using CorelDRAW Graphics Suite version 2024.

3. Results and discussion

3.1. Morphological and molecular characterization

***Xylaria chamelensis* Y. Osorio, R. Valenz., Hdz-Rdz., Raymundo, Hernández-García, sp. nov.**

Figure 1

MycoBank: MB861284

Etimology: "chamelensis" refers to the Estación de Biología Chamela, where this species was first collected.

Type: MEXICO, Jalisco State, La Huerta municipality, Chamela-Cuixmala Biosphere Reserve, Chamela

Table 2. Details of the sequences used for phylogenetic analysis.

Species	voucher	ITS	28S	β-tubulin	RPB2	Host/isolated from	Locality
Heteroxylaria oxyacanthae	859 JDR	GU322434	--	GQ495927	GQ844820	fallen fruits of *Crataegus monogyna*	USA
Heteroxylaria palmicola	604 PDD	GU322436	--	GQ495929	GQ844822	fruit	New Zealand
Hypoxylon fragiforme	MUCL 51264	KC477229	NG_066364	KX271282	MK887342	Epitype of *H. fragiforme*	Germany
Xylaria acuta	5220	JQ862676	JQ862637	JX868537	--	*Dendrobium* sp. root	China
Xylaria arbuscula	CBS126415	MH864101	MH875560	KX271257	KY624287	*Quercus* sp. fallen branch	Germany
Xylaria arbuscula	FL1030	OQ831957	--	KU684165	KU684247	*Cladonia evansii* thallus	USA
Xylaria arbuscula	89041211 (HAST)	GU300090	--	GQ478226	GQ844805	bark	Taiwan
Xylaria cf. *castorea*	91092303 (HAST)	GU324752	--	GQ502704	GQ853019	bark	Taiwan
Xylaria cf. *plebeja*	91122401 (HAST)	GU324740	--	GQ502689	GQ848353	*Machilus zuihoensis* trunk	Taiwan
"This study"	RV14508	PX401643	PX971233	PZ022449	PZ037936	Fabaceae fallen pod	Jalisco, Mexico
Xylaria cubensis	BCC 1027	AB625412	AB376683	AB625355	--	wood	Thailand
Xylaria cubensis	BCC 1144	AB625413	AB376701	AB625356	--	wood	Thailand
Xylaria curta	494 (HAST)	GU322444	--	GQ495937	GQ844831	dead wood	Martinique
Xylaria digitata	919 (HAST)	GU322456	--	GQ495949	GQ848338	wood	Ukraine
Xylaria feejeensis	92092013 (HAST)	GU322454	--	GQ495947	GQ848336	bark	Taiwan
Xylaria grammica	5151	JQ862665	JQ862626	JX868535	--	*Dendrobium* sp. root	China
Xylaria grammica	5228	JQ862677	JQ862638	JX868538	--	*Dendrobium* sp. root	China
Xylaria hypoxylon	95082001 (HAST)	GU300095	--	GQ487703	GQ844811	wood	Taiwan
Xylaria hypoxylon	152	GU300096	--	GQ260187	GQ844812	wood	Belgium
Xylaria intraflava	95060509 (HAST)	EU179866	--	GQ502718	GQ853035	ground of bamboo plantation	Taiwan
Xylaria longipes	CBS 148.73	KU683768	--	KU684204	KU684280	*Fagus silvatica* trunk	Germany
Xylaria multiplex	CMRP4983	ON325487	ON325575	ON803634	--	*Vochysia divergens* petiole	Brazil
Xylaria multiplex	580 (JF)	GU300098	--	GQ487705	GQ844814	dead wood	Martinique
Xylaria polymorpha	1012 (JDR)	GU322460	--	GQ495954	GQ848343	wood	USA
Xylaria scruposa	497 (JF)	GU322458	--	GQ495952	GQ848341	dead wood	Martinique
Xylaria telfairii	421 (JF)	GU324737	--	GQ502686	GQ848350	dead wood	Martinique
Xylaria venustula	FL0490	JQ760209	--	KU684143	--	*Cladonia didyma* thallus	USA

Biological Station, Búho Road. 19°27′02.1″N, 105°01′33.0″W. 100 m alt. September 17, 2011, R. Valenzuela 14508 (holotype: ENCB), ex-type: strain RV14508 (ENCB). GenBank Accession numbers: ITS PX401643; nrLSU PX971233; β-tubulin PZ037936; RPB2 PZ022449.

Diagnosis: Differs from *X. ianthinovelutina*, the most resembling pod-inhabitant species, by its smaller stromata, with a reddish-brown to dark brown surface, finely velutinate only at the stipe base, and olivaceous-brown to dark brown in color, equilateral wider ascospores (6–7 µm vs 4–5 µm wide).

Description: Stromata 17–40 mm long, and 2–4 mm wide, simple, gregarious, clavate-stipitate, straight, tapering toward the base, with fertile, rounded to rarely acute apices. The fertile portion is cylindrical, with exposed perithecial contours, 9–22 mm long and 2–4 mm wide; the surface is dark brown (8F5) to black, with some reddish-brown (8E5) tones; slightly wrinkled, carbonaceous. Stipes: well-defined, 8–17 mm length and 1 mm wide, straight to rolled up, sometimes presenting a swollen base, brownish orange (7C5) to brown (7E6), finely velutinate at the base. Outer layer or ectostroma: comprises a thin, black-carbonaceous crust, 200–400 µm thick, with epidermoidea texture, composed of 5–6 µm wide, thick-walled hyphae, light olivaceous-brown. Endostroma: soft, fleshy, pinkish white (5C3) to pale yellow (5B3) at the center, solid, spongy to compact, not turning hollow upon drying, with intricate texture, composed of 5–6 µm wide thick-walled hyphae, hyaline to light yellow. Perithecia: 0.3–0.47 × 0.32–0.35 mm (n = 40) in diameter, subglobose to obovoid, immersed, irregularly distributed in several layers observed in a cross-section view, thick-walled, shiny black, carbonaceous, and ostioles slightly papillated, black. Asci: 200–210 × 7.5–8.0 µm (n = 30), cylindrical, stipitate, octosporic, with apical apparatus 0.5–1 × 1.5–2.0 µm, tubular, amyloid in Melzer's reagent. Ascospores: (11.0–) 12.0–13.0 (–14.0) × 6.0–7.0 µm (Q = 1.92, n = 40), uniseriate, ellipsoid-equilateral, with broadly-rounded ends, olivaceous-brown to dark brown, unicellular, smooth, with straight to slightly

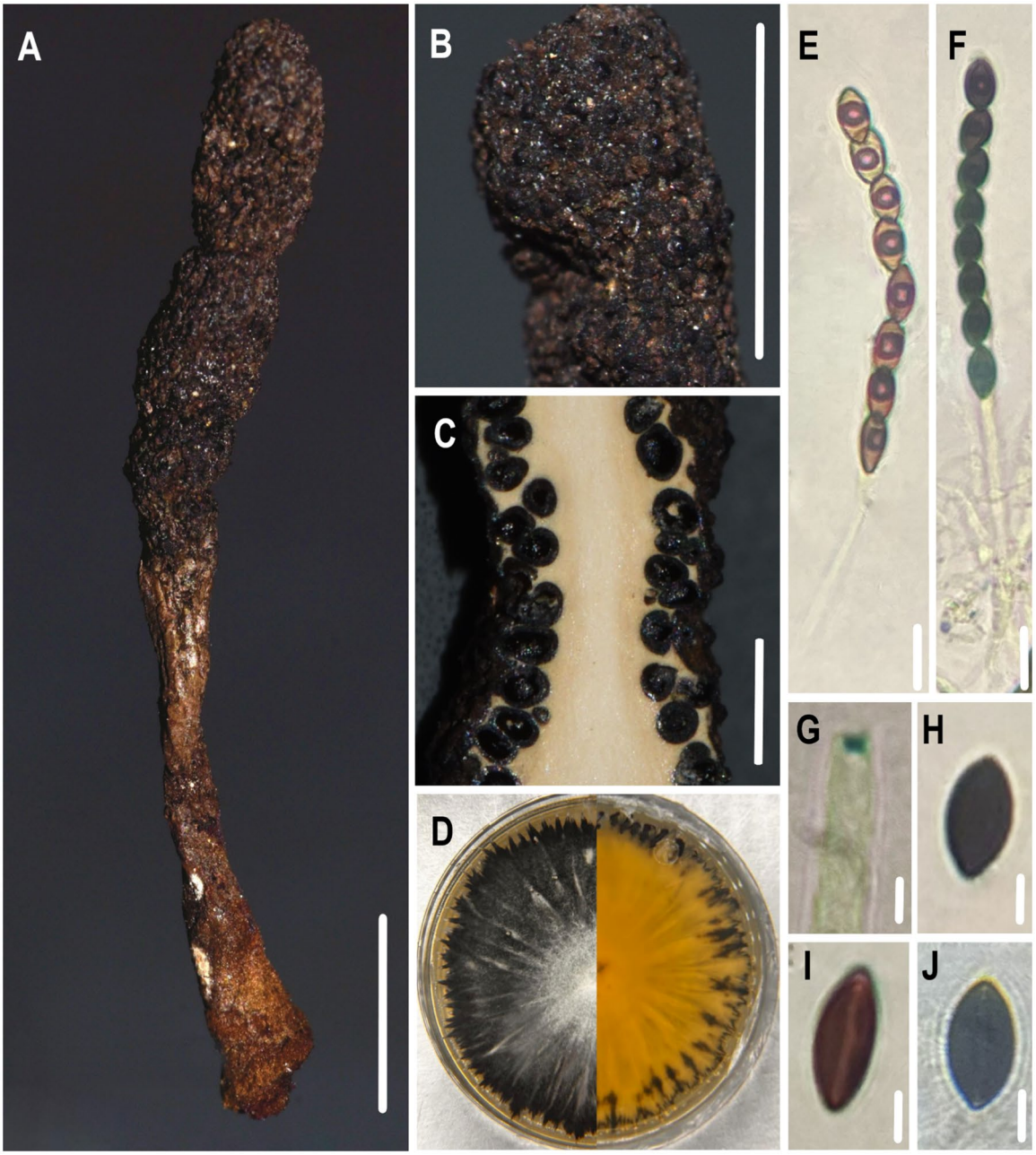

Figure 1. Morphological characteristics of *Xylaria chamelensis* sp. nov. (A) Stroma; (B) Closer view of the ectostroma; (C) Endostroma and perithecia in cross-section view; (D) Aerial and substrate mycelium color on PDA after 15 d of incubation at 28 °C; (E) Asci with immature ascospores; (F) Asci with mature ascospores; (G) Amyloidal apical pore; (H) Ascospore; (I–J) Ascospores showing the germinal line. Scale bars A,B: 5 mm, C: 1 mm, E,F: 20 µm, G–J: 5 µm.

sigmoid germ line, almost spore-length, immature ascospores show a single guttula almost spore-length, no hyaline sheath was observed on negative stain.

Cultural characteristics: After 15 d on PDA, colonies fill up a 50 mm Petri dish at 25 °C. They are initially whitish and later become black toward the margins, with dense aerial mycelium. The colony margins are covered with numerous, small, sterile, simple stromata-like structures that end in white tips. The reverse of the colony is zonate, with pale brown furrows, and displays a black margin. Neither conidia nor conidiophores were observed, even after incubation for 45 d.

Habitat: Growing on fallen Fabaceae pods in tropical dry forest.

Distribution: Currently known from the type locality in the state of Jalisco, Mexico. The Chamela Biological Station is located within a Protected Natural Area where only authorized research is permitted. Given the minimal anthropogenic disturbance in this region, the population of *X. chamelensis* is expected to remain stable in-situ.

Additionally examined material: MEXICO. State of Jalisco, La Huerta municipality, Chamela-Cuixmala Biosphere Reserve, Chamela Biological Station, Búho

Road. 19°27′02″N, 105°01′33″W. 100 m alt. September 17, 2011, R. Valenzuela 14494 (ENCB).

Taxonomic notes: *Xylaria chamelensis* is characterized by having small, slender, gregarious stromata with a cylindrical fertile portion and a well-defined stipe. The fertile portion is dark brown to black, where some reddish-brown tones are evident. The stipe is finely velutinate only at the base. The ellipsoid-equilateral ascospores are consistently olivaceous-brown to dark brown, exhibiting a straight to slightly sigmoidal germ line that nearly spans the entire spore length. *Xylaria scruposa* is morphologically similar to *X. chamelensis* by displaying an unbranched stroma, clavate-stipitate, with a wooly tomentum, conspicuous ostioles, and ascospores with a slightly sigmoidal ventral germ slit less than spore-length (15.7–24.1 × 5.4–8.1 µm) [30,31]; still, *X. chamelensis* only grows on Fabaceae pods, lacks the polygonal to elongated scales that differentiate it from the stromatal outer layer, and has smaller equilateral ascospores (12.0–13.0 (–14.0) × 6.0–7.0 µm). Another similar species is *Xylaria feejeensis* (Berk.) Fr. by the unbranched, cylindrical, gregarious stromata, reddish brown, with perithecial mounds barely exposed, ascal apical apparatus wider than high, and ellipsoid ascospores with a germ slit almost spore-length; however they can be differentiated because *X. chamelensis* has larger ascospores (12.0–13.0 × 6.0–7.0 µm vs 8.2–10.6 × 4.4–5.1 µm) and lacks the cellular appendage somehow mucilaginous that can be observed on negative stains of *X. feejeensis* ascospores [31].

Other species that grow on Fabaceae pods are *Xylaria culleniae* Berk. & Broome, *Xylaria fabacearum* R.H. Perera, E.B.G. Jones & K.D. Hyde, and *Xylaria microcarpa* Hai X. Ma & Yu Li. Still, *X. chamelensis* only has simple stromata, velutinate at the stipe base; in contrast with the stromata of *X. fabacearum* that can be branched and lack a tomentum [32], while *X. microcarpa* and *X. culleniae* have tomentose stromatal surfaces. *X. chamelensis* differs from these species by having olivaceous brown to dark brown ascospores with a germ slit that is sometimes slightly sigmoidal, in contrast to light brown ascospores with a straight germ slit in *X. microcarpa*. Moreover, *X. chamelensis* ascospores lack a hyaline sheath, which is present in *X. culleniae* ascospores [33].

3.2. Genome assembly and annotation

Whole-genome sequencing of *Xylaria chamelensis* sp. nov. strain RV14508 generated 47,268,426 raw reads, with an average length of 150 bp, and a 45.09% GC content. After quality evaluation and filtering, 47,073,990 high-quality reads were retained. The final reference-guided assembly yielded a total genome size of 51.93 Mbp with a GC content of 42.34%. Through the scaffolding process and length filtering (≥ 1000 bp), the assembly was consolidated into 3,364 contigs, significantly improving continuity metrics. Comprehensive genome assembly statistics are summarized in Table 3.

The BUSCO analysis against the xylariales_odb12 lineage revealed a completeness of 98.5% (5620 out of 5708 total groups). Specifically, 98.4% (5618) of the BUSCOs were identified as complete and single-copy, whereas only 0.2% were fragmented and 1.3% were missing (Supplementary Figure 1). The absence of significant duplication suggests a high-quality haploid assembly with minimal redundancy or contamination. The genome contains 11,238 predicted protein-coding genes and exhibits high structural integrity, with no major misassemblies detected. These metrics indicate that the assembly captures most of the coding potential of a *Xylaria* fungus, despite the inherent fragmentation of short-read sequencing.

3.3. Biosynthetic gene cluster analysis and CAZyme analysis

Over 70 putative BGCs were detected by fungiSMASH, primarily classified as encoding terpene, non-ribosomal peptide synthetase (NRPS), and Type I Polyketide synthase (T1PKS), although this analysis identified only seven with high similarity confidence (Table 4). Those clusters are likely responsible for producing aspulvinone B/H, choline, dimethylcoprogen, clavaric acid, fusarin C, and mellein. Aspulvinone B/H are fungal molecules isolated from *Aspergillus* spp., which have exhibited antibacterial and cytotoxic activities [34]. Choline is a metabolite, essential for the growth of filamentous fungi, that serves as a component of the major membrane phospholipid and of the sulfate ester in sulfate metabolism [35]. Dimethylcoprogen is a fungal non-ribosomal peptide siderophore that enhances growth and controls the

Table 3. Assembly statistics of *Xylaria chamelensis* strain RV14508 genome.

Attributes	*De novo* assembly	Referenced assembly
Number of reads	47,073,990 bp	51,936,471 bp
Number of contigs	5,016	3,364
Sequence coverage	133×	136×
Genome size	52.2 Mb	51.9 Mb
% GC	41.93	42.34
Largest contig	492,740	2,154,935
N50 contigs size	88,764	452,556
N90 contigs size	2915	4375
L50	157	32
Predicted protein-coding genes	9,310	11,238
BUSCO completeness (%)	98.4	98.5

Table 4. Putative BGCs of secondary metabolites of *Xylaria chamelensis* strain RV14508 detected by fungiSMASH.

Region	Type	Chromosome location	Most similar known cluster	Activity	Similitude coverage (%)
32.1	T1PKS	30,264–95,865	FR901512	Unknown	74%
35.1	NRPS-like	1–57,290	Choline	Component of the major membrane phospholipid	100%
53.1	NRPS	41,620–106,905	Dimethylcoprogen	Siderophore	99%
132.1	T1PKS	1–18,878	Fusarin C	Unknown	68%
141.1	NRPS-like	1–37,132	Aspulvinone B1/Aspulvinone H	Antibacterial, Cytotoxic	98%
147.1	Terpene	63,038–91,785	Clavaric acid	Antitumoral	94%
224.1	T1PKS	1–57,346	(-)-Mellein	Phytotoxic	98%

NRPS: non-ribosomal peptide synthetase; T1PKS: Type I Polyketide synthase.

development of other microorganisms in the environment [36]. Meanwhile, BGCs that produce clavaric acid and mellein are found in fungi and in other organisms, such as cyanobacteria and plants, where they exhibit antitumoral and phytotoxic activities, respectively [37,38]. Finally, fusarins are polyketides produced by *Fusarium* spp. and *Metarhizium anisopliae* (Metschn.) Sorokin [39]. Fusarin C is a mycotoxin produced by several *Fusarium* species and is considered a mutagenic compound, as it has been associated with various cancers, although it has been cited to have mycoestrogenic properties [40,41].

These *in silico* results offer a valuable preliminary map for understanding the gene distribution within *Xylaria* groups, a critical foundation for future functional studies of metabolic pathways and provide a useful dataset for comparing genetic diversity across the genus and related taxa, facilitating a deeper understanding of evolutionary trends in the Xylariales.

On the other hand, 496 genes were identified as CAZymes, yielding 504 modules classified into six classes: 246 GHs representing (47.67%) of the total, followed by 135 auxiliary activities (AAs, 26.16%), 51 GTs, 40 CEs, 17 CBMs, and 15 PLs.

The CAZymes repertoire found in this analysis is indicative of potential high metabolic versatility, primarily associated with the degradation of lignocellulosic material. The highest percentage was found in those related to GHs and AAs CAZymes genes, suggesting a putative role in the hydrolysis and oxidation of plant polysaccharides. This is consistent with the isolation source of the fungal strain – fallen fruits – which represent a habitat rich in simple and complex carbohydrates. Furthermore, the diversity of AAs, particularly from the AA1, AA3, and AA9 subfamilies, highlights significant ligninolytic potential that could facilitate carbon acquisition from phenolic compounds. This enzymatic profile is typically broadly distributed among fungi with facultative xylophagous saprotrophic nutrition, especially those capable of alternating between mutualistic associations and the degradation of decaying plant material [42,43].

The MEROPS database yielded 360 protease genes, grouped into five catalytic types (Table 5), with a

Table 5. Identified proteases from the *Xylaria chamelensis* genome strain RV14508 by the MEROPS database.

Catalytic type	Families (number of genes)
Serine (S)	S08: subtilisine (2)
	S09: prolil-oligopeptidases (7)
	S10: carboxypeptidases (5)
Aspartic (A)	A01: pepsins (5)
Metallo-proteases (M)	M14: carboxypeptidases A/B zinc-dependent (2)
	M24: methionineo-aminopeptidases (1)
	M28: amino- and carboxi-peptidases (3)
Threonine (T)	T01: proteasome (4)
Cysteine (C)	C01: papain (2)
	C19: ubiquitine-specific (1)

predominance of serine peptidases (S09, S10), as observed in ascomycete fungi, suggesting the presence of a versatile proteolytic machinery capable of breaking down a wide range of protein substrates within the annotated genome of *X. chamelensis*. The role of extracellular proteolysis in nitrogen acquisition has been described as central to obtaining this essential macroelement from a poor nitrogen source, as might be expected from a fallen fruit [44]. Meanwhile, aspartic proteases and metalloproteases may be involved in the post-translational maturation of secreted enzymes and cell wall remodeling, processes relevant to substrate colonization and utilization [45,46]. Peptidases that use serine in their active site are the most abundant in the annotated genome of *X. chamelensis*. The abundance of S09 enzymes suggests that this strain can degrade proteins rich in proline, and S10 enzymes have been reported as being involved in protein digestion [47]. Metallo- and aspartic peptidases, such as A01, are commonly reported in fungi; they remain active under acidic conditions because these organisms secrete enzymes into the environment to meet their nutritional requirements [44]. Threonine peptidases form multiprotein complexes such as proteasome. In contrast, the least represented, cysteine peptidases (C19) and M24, could be involved in nutrient vacuolar mobilization and post-translational maturation, respectively [48–50].

The peptidase profile and the CAZyme diversity found in *X. chamelensis* strains reveal a putative specialization in peptide hydrolysis (with a dominance of enzymes that use serine in their active sites) and establish that this fungal species has a metabolism potentially oriented toward processing structural

proteins and degrading macromolecules present in plant material. As a saprotrophic organism from fallen fruits, the genomic profile reveals an evolutionary adaptation to this habitat, providing it with a competitive advantage in this ecological niche. Therefore, it can be a likely resource for biotechnological applications involving the degradation and transformation of complex polymers, such as cellulose, hemicellulose, and lignin-derived phenolic compounds.

Nevertheless, these results should be interpreted with caution, as they were derived *in silico*; experimental validation is necessary to confirm these putative functions and support further discussion.

3.4. Phylogenomic approach

The analysis included 27 annotated genomes, yielding 4420 orthogroups with 3218 single-copy orthogroups. The phylogenomic reconstruction produced a well-supported phylogenomic tree, with most branches displaying high support (>95% bootstrap), as seen in Figure 2. The tree includes representatives from three main clades within the *Xylaria* s.l. in the Xylariaceae: *Xylaria hypoxylon*-related clade (HY), *Xylaria polymorpha*-related clade (PO), and *Xylaria* termite-associated clade (TE). To assess the robustness of the amino acid-based phylogenomic reconstruction, we compare it with a multi-locus phylogeny of *Xylaria* sequences (Figure 3). These analyses support the polyphyletic nature of the genus, as demonstrated in prior studies [3,8,51,52], and retrieved a similar topology in which *X. chamelensis* forms a well-supported clade with *Xylaria feejeensis,* both included in the PO clade.

Species from the PO clade are represented by *X. cubensis* aggregate, *X. longipes* aggregate, and *X. polymorpha* aggregate; most of these taxa have stromata with a fertile, blunt apex, except for the fructicolous/follicolous or penzigioid species, which can be sessile to stipitate with a fertile or sterile apex, and other diagnostic stromatal features can include whether an outer stromatal layer persists into maturity or not [2]. In multigene reconstruction, most species associated with fallen fruits/seeds are basal to the PO clade, such as *X. oxyacanthae* or *Xylaria palmicola* G. Winter [3]. Other authors have included species of *Xylaria* growing on fruits in the basal IA clade, adding *X. ianthinovelutina* or *Xylaria juruensis* Henn (≡*Neoxylaria juruensis* S. Konta & K.D. Hyde). Currently, the genus *Neoxylaria* has been segregated to include palm-related *Xylaria* species, which form conspicuously exposed perithecial contours under a narrowly striped outer layer [53]; meanwhile, *Heteroxylaria* has been erected to include *Xylaria* species characterized by having cylindrical, dark stromata and growing on the nutshell of fruits, with *H. oxyacanthae* as the type species [8].

Regarding the strains used in this amino acid-based phylogenomic reconstruction, a previous

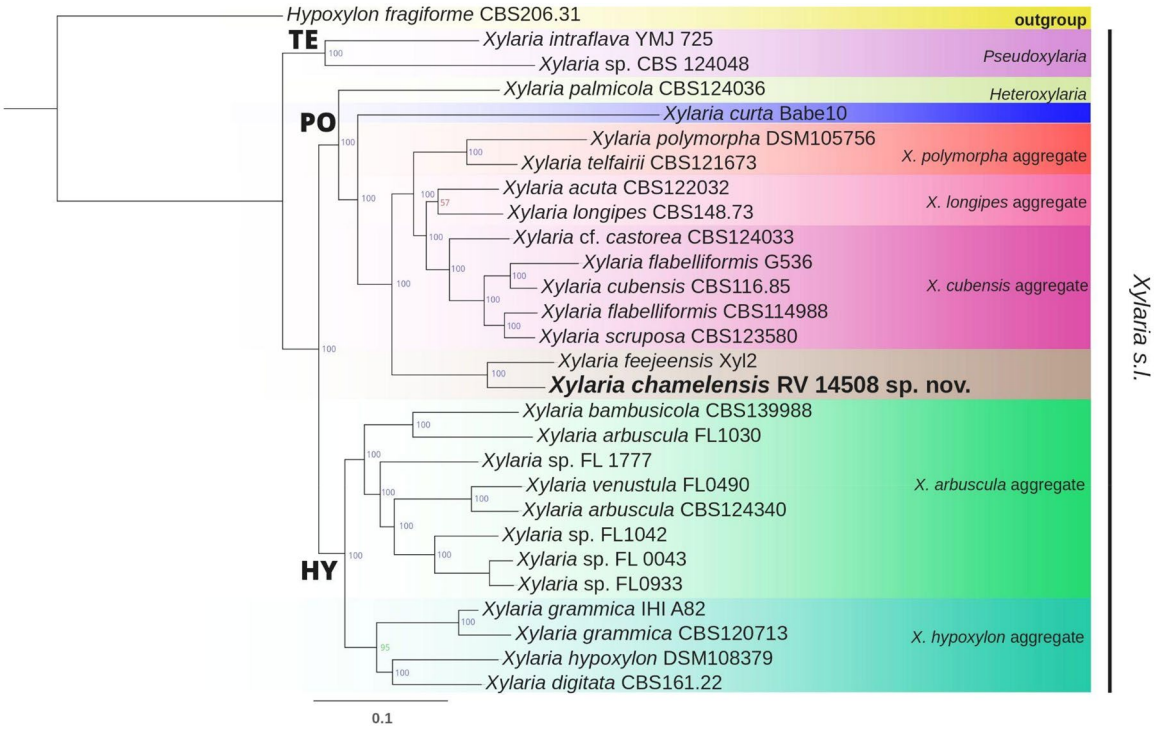

Figure 2. Phylogenomic ML tree based on single-copy orthologous genes for the *Xylaria chamelensis* strain RV14508 (in bold) and related *Xylaria* genomes. Bootstrap values from 1000 replications are shown at the nodes. *Xylaria s.l.*: *Xylaria sensu lato*. *Xylaria hypoxylon*-related clade (HY), *Xylaria polymorpha*-related clade (PO), and *Xylaria* termite-related clade (TE).

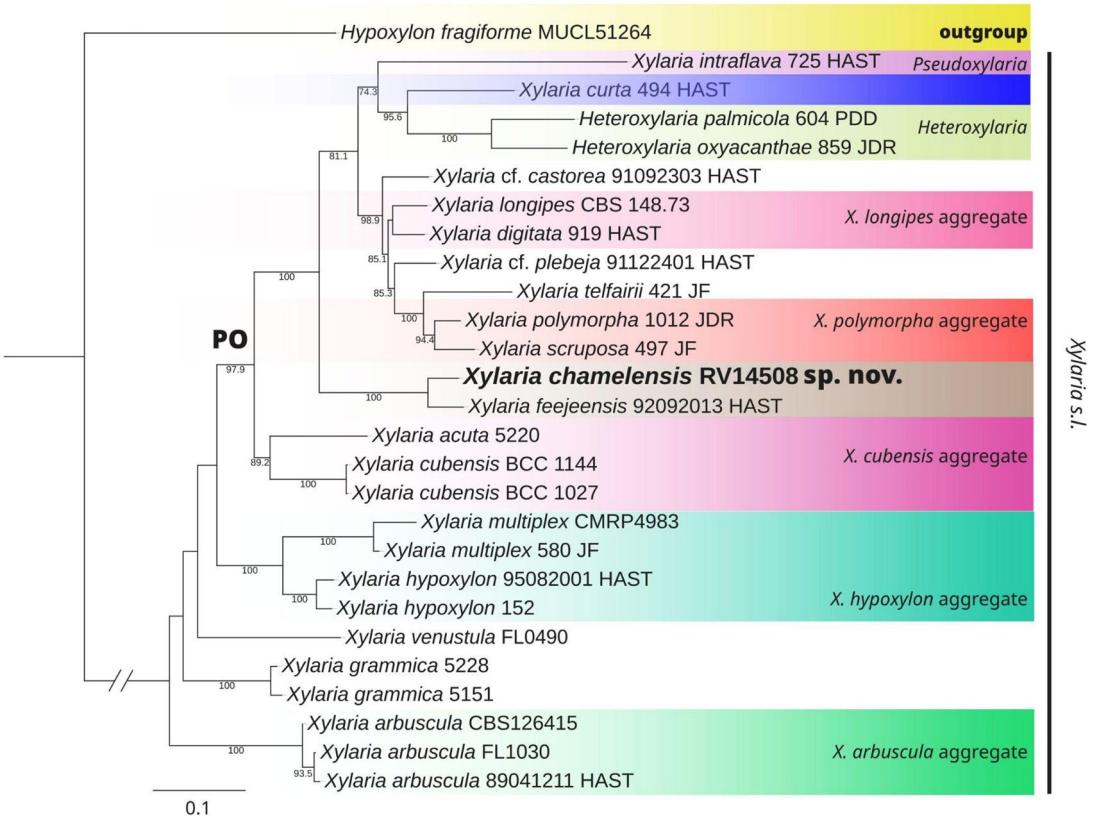

Figure 3. Phylogenetic ML multilocus tree based on ITS-nrLSU-RPB2-β-tubulin concatenated markers for the *Xylaria chamelensis* strain RV14508 (in bold) and related *Xylaria* species. Bootstrap values from 1000 replications are shown at the nodes. *Xylaria s.l.*: *Xylaria sensu lato* and *Xylaria polymorpha*-related clade (PO).

study [54] noted that *Xylaria* CBS114988 (accession number: GCA_022495235.1) was morphologically identified as *Xylaria curta* Fr., but the phylogenetic position of the isolate based on the ITS-LSU nrDNA region coincided with those reported for *Xylaria flabelliformis* (Schwein.) Berk. & M.A. Curtis; therefore, is named here as *X. flabelliformis*, a species grouped within *X. cubensis* aggregate by having a thick carbonaceous layer immediately beneath the ectostromata and stromatal surface smooth. Also, *X. palmicola* (≡*Heteroxylaria palmicola* (G. Winter) Hai X. Ma, A.H. Zhu & Y. Li) strain CBS124036 is a representative of *Heteroxylaria*, and is related to the PO clade, as previously noted for *X. curta*, *X. feejeensis*, and *X. palmicola.* The strains of *X. curta* (accession number: GCA_027595895.1) and *X. feejeensis* (accession number: GCA_051622775.1) used in this analysis were isolated from deciduous deadwood in Vietnam. Notably, X. *feejeensis* showed a close relationship with the *X. chamelensis* strain RV14508, which in turn is related to *X. corniformis*, a connection also observed for *X. curta* and *X. feejeensis* in other studies [3,8].

In both analyses, *X. chamelensis* was closely related to *X. feejeensis*. They share similar morphological features, as discussed in the taxonomic notes, but can be differentiated with a polyphasic approach. *X. feejeensis* is a widespread tropical species with great morphology variability considering a complex of taxa; however, here only the features included in its type description [30,31] were used. Moreover, previous studies have noted phylogenetic differences between materials of *X. feejeensis* from the Neotropics and the Paleotropics, highlighting the difficulty to assess them only on morphology-based studies [3]. Thus, *X. chamelensis* is proposed as a distinct, independent lineage, supporting that this specimen represents a new species. Furthermore, other studies determine that the TE clade is a well-described monophyletic clade comprising only *Xylaria* termite-associated species [52], and it was segregated as the subgenus *Pseudoxylaria* [3], represented herein by *Xylaria intraflava* Y.M. Ju & H.M. Hsieh and *Xylaria* sp. CBS124048, both isolated from termite nests. Finally, the clade HY is defined as the aggregate that includes the type species *Xylaria hypoxylon* (L.). Grev., and those *Xylaria* species that belong to *X. arbuscula* aggregate, characterized by cylindrical stromata with a pointed apex and a persisting peeling layer on the stromatal surface, and these are considered as *Xylaria* sensu stricto; however, the study of the phylogenetic position of the clades within the genus has not reached a consensus. Therefore, *Xylaria* sensu lato remains a polyphyletic genus and is used to group clades *Xylaria*-like that have not been traditionally named.

Phylogenomic analysis enhances phylogenetic accuracy by using extensive gene data from multiple, independently evolving regions of the genome; thus, it maximizes information content and deepens our understanding of phylogenies at the species level and even within major clades [55]. In conclusion, genomic data, such as the information provided here, serve as a valuable resource for genome-based taxonomy, not only increasing our understanding of fungal systematics but also offering new insights into speciation and diversity, while revealing the biosynthetic potential of fungal species [56].

Acknowledgments

YO-N thanks the Postgrad in CQB from the Escuela Nacional de Ciencias Biológicas (IPN), and the SECIHTI scholarship.

Disclosure statement

The authors declare no known competing financial interests or personal relationships that could have influenced the work reported in this article.

Funding

This research was funded by Secretaría de Investigación y Posgrado (SIP) of the Instituto Politécnico Nacional (IPN), through projects SIP 20251037, 20251163, 20254302, 20251281, 20260423, and 20260756. IPICyT's National Supercomputing Center supported this research with the computational time grant TKII-E-1025-I-101025-81/PR-91.

ORCID

Yulena Osorio-Navarro http://orcid.org/0000-0003-0241-8534
Ricardo Valenzuela http://orcid.org/0000-0001-6596-5223
César Hernández-Rodríguez http://orcid.org/0000-0003-2411-9789
Tania Raymundo http://orcid.org/0000-0002-7525-0034
Abigail Pérez-Valdespino http://orcid.org/0000-0002-2885-592X
Hannya Chamorro-Martínez http://orcid.org/0000-0002-6702-9479
Juan Alfredo Hernández-García http://orcid.org/0000-0001-7094-7900

Data availability statement

This Whole Genome Shotgun project has been deposited at DDBJ/ENA/GenBank under the accession JBSWBP000000000. The version described in this paper is the second release.

The associated BioProject accession number is PRJNA1338710. The associated BioSample accession number is SAMN52580428. The GenBank number accession is GCA_056151845.

References

[1] Whalley AJS. The xylariaceous way of life. Mycol Res. 1996;100(8):897–922. doi:10.1016/S0953-7562(96)80042-6.
[2] Ju YM, Hsieh HM. *Xylaria* species associated with fallen leaves and petioles. Bot Stud. 2023a;64(1):19. doi:10.1186/s40529-023-00377-w.
[3] Hsieh HM, Lin CR, Fang MJ, et al. Phylogenetic status of *Xylaria* subgenus *Pseudoxylaria* among taxa of the subfamily Xylarioideae (Xylariaceae) and phylogeny of the taxa involved in the subfamily. Mol Phylogenet Evol. 2010;54(3):957–969. doi:10.1016/j.ympev.2009.12.015.
[4] Suwannasai N, Sangvichien E, Phosri C, et al. Exploring the Xylariaceae and its relatives. Bot Stud. 2023;64(1):15. doi:10.1186/s40529-023-00389-6.
[5] Chen YP, Su PW, Hyde KD, et al. Phylogenomics and diversification of Sordariomycetes. Mycosphere. 2023;14(1):414–451. doi:10.5943/mycosphere/14/1/5.
[6] Helaly SE, Thongbai B, Stadler M. Diversity of biologically active secondary metabolites from endophytic and saprotrophic fungi of the ascomycete order Xylariales. Nat Prod Rep. 2018;35(9):992–1014. doi:10.1039/c8np00010g.
[7] Wibberg D, Stadler M, Lambert C, et al. High-quality genome sequences of thirteen Hypoxylaceae (Ascomycota) strengthen the phylogenetic family backbone and enable the discovery of new taxa. Fungal Divers. 2021;106(1):7–28. doi:10.1007/s13225-020-00447-5.
[8] Zhu AH, Song ZK, Wang JF, et al. Multi-gene phylogenetic analyses reveals *Heteroxylaria* gen. Nov. and new contributions to xylariaceae (Ascomycota) from China. JoF. 2024;10(9):645. doi:10.3390/jof10090645.
[9] Munsell® Soil Color Chart. Revised edition. Macbeth division of Kollmorgen instruments corporation 405. New York: New Windsor; 1994.
[10] Allers T, Lichten M. A method for preparing genomic DNA that restrains branch migration of Holliday junctions. Nucleic Acids Res. 2000;28(2):e6-e6–6. doi:10.1093/nar/28.2.e6.
[11] White TJ, Bruns T, Lee S, et al. Amplification and direct sequencing of ribosomal RNA genes for phylogenetics. In: Innis MA, Gelfand DH, Sninsky KY, White TJ, editors. PCR Protocols, a Guide to Methods and Applications. New York: Academic Press; 1990. p. 315–322.
[12] Vilgalys R, Hester M. Rapid genetic identification and mapping of enzymatically amplified ribosomal DNA from several *Cryptococcus* species. J Bacteriol. 1990;172(8):4238–4246. doi:10.1128/jb.172.8.4238-4246.1990.
[13] Altschul SF, Gish W, Miller W, et al. Basic local alignment search tool. J Mol Biol. 1990;215(3):403–410. doi:10.1016/S0022-2836(05)80360-2.
[14] Bankevich A, Nurk S, Antipov D, et al. SPAdes: a new genome assembly algorithm and its applications to single-cell sequencing. J Comput Biol. 2012;19(5):455–477. doi:10.1089/cmb.2012.0021.
[15] Gurevich A, Saveliev V, Vyahhi N, et al. QUAST: quality assessment tool for genome assemblies. Bioinformatics. 2013;29(8):1072–1075. doi:10.1093/bioinformatics/btt086.

[16] Alonge M, Soyk S, Ramakrishnan S, et al. RaGOO: fast and accurate reference-guided scaffolding of draft genomes. Genome Biol. 2019;20(1):1–17. doi:10.1186/s13059-019-1829-6.
[17] Shen W, Le S, Li Y, et al. SeqKit: a cross-platform and ultrafast toolkit for FASTA/Q file manipulation. PLoS One. 2016;11(10):e0163962. doi:10.1371/journal.pone.0163962.
[18] Simão FA, Waterhouse RM, Ioannidis P, et al. BUSCO: assessing genome assembly and annotation completeness with single-copy orthologs. Bioinformatics. 2015;31(19):3210–3212. doi:10.1093/bioinformatics/btv351.
[19] Stanke M, Steinkamp R, Waack S, et al. AUGUSTUS: a web server for gene finding in eukaryotes. Nucleic Acids Res. 2004;32:W309–W312. doi:10.1093/nar/gkh379.
[20] Blin K, Shaw S, Vader L, et al. antiSMASH 8.0: extended gene cluster detection capabilities and analyses of chemistry, enzymology, and regulation. Nucleic Acids Res. 2025;53(W1):W32–W38. doi:10.1093/nar/gkaf334.
[21] Zhang H, Yohe T, Huang L, et al. dbCAN2: a meta server for automated carbohydrate-active enzyme annotation. Nucleic Acids Res. 2018;46(W1):W95–W101. doi:10.1093/nar/gky418.
[22] Lombard V, Golaconda Ramulu H, Drula E, et al. The carbohydrate-active enzymes database (CAZy) in 2013. Nucleic Acids Res. 2014;42:D490–D495. doi:10.1093/nar/gkt1178.
[23] Stewart RD, Auffret MD, Warr A, et al. Compendium of 4,941 rumen metagenome-assembled genomes for rumen microbiome biology and enzyme discovery. Nat Biotechnol. 2019;37(8):953–961. [31375809].
[24] Rawlings ND, Waller M, Barrett AJ, et al. MEROPS: the database of proteolytic enzymes, their substrates and inhibitors. Nucleic Acids Res. 2014;42:D503–D509. doi:10.1093/nar/gkt953.
[25] Emms DM, Kelly S. OrthoFinder: solving fundamental biases in whole genome comparisons dramatically improves orthogroup inference accuracy. Genome Biol. 2015;16(1):157. doi:10.1186/s13059-015-0721-2.
[26] Nguyen LT, Schmidt HA, Von Haeseler A, et al. IQ-TREE: a fast and effective stochastic algorithm for estimating maximum-Likelihood phylogenies. Mol Biol Evol. 2015;32(1):268–274. doi:10.1093/molbev/msu300.
[27] Kalyaanamoorthy S, Minh BQ, Wong TK, et al. ModelFinder: fast model selection for accurate phylogenetic estimates. Nat Methods. 2017;14(6):587–589. doi:10.1038/nmeth.4285.
[28] Guindon S, Dufayard J-F, Lefort V, et al. New algorithms and methods to estimate maximum-likelihood phylogenies: assessing the performance of PhyML 3.0. Syst Biol. 2010;59(3):307–321. doi:10.1093/sysbio/syq010.
[29] Rambaut A. Institute of evolutionary biology. Edinburgh, Scotland: University of Edinburgh; 2018. Available from: https://tree.bio.ed.ac.uk/software/figtree
[30] Fournier J, Lechat C, Courtecuisse R. The genus *Xylaria* sensu lato (Xylariaceae) in Guadeloupe and Martinique (French West Indies) II. Taxa with robust upright stromata. Ascomycete.org. 2019;11(3):77–115.
[31] Fournier J, Lechat C, Courtecuisse R. The genus *Xylaria* sensu lato (Xylariaceae) in Guadeloupe and Martinique (French West Indies) III. Taxa with slender upright stromata. Ascomycete.org. 2020;12(3):81–164.
[32] Perera RH, Hyde KD, Maharachchikumbura SSN, et al. Fungi on wild seeds and fruits. Mycosphere. 2020;11(1):2108–2480. doi:10.5943/mycosphere/11/1/14.
[33] Ju YM, Rogers JD, Hsieh HM. *Xylaria* species associated with fallen fruits and seeds. Mycologia. 2018;110(4):726–749. doi:10.1080/00275514.2018.1469879.
[34] Machado FP, Kumla D, Pereira JA, et al. Prenylated phenylbutyrolactones from cultures of a marine sponge-associated fungus, *Aspergillus flavipes* KUFA1152. Phytochemistry. 2021;185:112709. [33636575]
[35] Markham P, Robson GD, Bainbridge BW, et al. Choline: its role in the growth of filamentous fungi and the regulation of mycelial morphology. FEMS Microbiol Rev. 1993;10(3–4):287–300. doi:10.1111/j.1574-6968.1993.tb05872.x.
[36] Renshaw JC, Robson GD, Trinci AP, et al. Fungal siderophores: structures, functions, and applications. Mycol Res. 2002;106(10):1123–1142. doi:10.1017/S0953756202006548.
[37] Godio RP, Martín JF. Modified oxidosqualene cyclases in the formation of bioactive secondary metabolites: biosynthesis of the antitumor clavaric acid. Fungal Genet Biol. 2009;46(3):232–242. doi:10.1016/j.fgb.2008.12.002.
[38] Reveglia P, Savocchia S, Billones-Baaijens R, et al. Spencertoxin and spencer acid, new phytotoxic derivatives of diacrylic acid and dipyridinbutan-1, 4-diol produced by *Spencermartinsia viticola*, a causal agent of grapevine *Botryosphaeria dieback* in Australia. Arabian J Chem. 2020;13(1):1803–1808. doi:10.1016/j.arabjc.2018.01.014.
[39] Krasnoff SB, Sommers CH, Moon YS, et al. Production of mutagenic metabolites by *Metarhizium anisopliae*. J Agric Food Chem. 2006;54(19):7083–7088. doi:10.1021/jf061405r.
[40] Niehaus EM, Diaz-Sanchez V, von Bargen KW, et al. Fusarins and fusaric acid in *Fusaria*. Biosynthesis and molecular genetics of fungal secondary metabolites. New York: Springer New York; 2014. doi:10.1007/978-1-4939-1191-2_11.
[41] Sondergaard TE, Hansen FT, Purup S, et al. Fusarin C acts like an estrogenic agonist and stimulates breast cancer cells in vitro. Toxicol Lett. 2011;205(2):116–121. doi:10.1016/j.toxlet.2011.05.1029.
[42] Treseder KK, Lennon JT. Fungal traits that drive ecosystem dynamics on land. Microbiol Mol Biol Rev. 2015;79(2):243–262. doi:10.1128/MMBR.00001-15.
[43] Miyauchi S, Kiss E, Kuo A, et al. Large-scale genome sequencing of mycorrhizal fungi provides insights into the early evolution of symbiotic traits. Nat Commun. 2020;11(1):5125. doi:10.1038/s41467-020-18795-w.
[44] Semenova TA, Dunaevsky YE, Beljakova GA, et al. Extracellular peptidases as possible markers of fungal ecology. Appl Soil Ecol. 2017;113:1–10. doi:10.1016/j.apsoil.2017.01.002.
[45] Karlsson M, Atanasova L, Jensen DF, et al. Necrotrophic mycoparasites and their genomes. Microbiol Spectr. 2017;5(2):10–1128. doi:10.1128/microbiolspec.FUNK-0016-2016.
[46] Allen CC, Díaz-Escandón D, DeLong-Duhon S, et al. Massive gene loss in the fungus *Sporothrix epigloea* accompanied a shift to life in a glucuronoxylomannan-based

gel matrix. Genome Biol Evol. 2025;17(2):evaf015. doi:10.1093/gbe/evaf015.

[47] Chen WT, Kelly T, Ghersi G. DPPIV, seprase, and related serine peptidases in multiple cellular functions. Curr Top Dev Biol. 2003;54:207–232. doi:10.1016/s0070-2153(03)54010-8.

[48] Hatsugai N, Kuroyanagi M, Yamada K, et al. A plant vacuolar protease, VPE, mediates virus-induced hypersensitive cell death. Science. 2004;305(5685):855–858. doi:10.1126/science.1099859.

[49] Hatsugai N, Iwasaki S, Tamura K, et al. A novel membrane fusion-mediated plant immunity against bacterial pathogens. Genes Dev. 2009;23(21):2496–2506. doi:10.1101/gad.1825209.

[50] Page MJ, Di Cera E. Serine peptidases: classification, structure and function. Cell Mol Life Sci. 2008;65(7–8):1220–1236. doi:10.1007/s00018-008-7565-9.

[51] Pan XY, Song ZK, Qu Z, et al. Three new *Xylaria* species (Xylariaceae, Xylariales) on fallen leaves from Hainan Tropical Rainforest National Park. MycoKeys. 2022;86:47–63. doi:10.3897/mycokeys.86.71623.

[52] Ju YM, Hsieh HM, Suwannasai N. *Xylaria furcata* reconsidered and nine resembling species. Bot Stud. 2023b;64(1):21. doi:10.1186/s40529-023-00392-x.

[53] Konta S, Hyde KD, Phookamsak R, et al. Polyphyletic genera in Xylariaceae (Xylariales): *Neoxylaria* gen. nov. and *Stilbohypoxylon*. Mycosphere. 2020;11(1):2629–2651. doi:10.5943/mycosphere/11/1/17.

[54] Franco ME, Wisecaver JH, Arnold AE, et al. Ecological generalism drives hyperdiversity of secondary metabolite gene clusters in xylarialean endophytes. New Phytol. 2022;233(3):1317–1330. doi:10.1111/nph.17873.

[55] Zhang N, Luo J, Bhattacharya D. Advances in fungal phylogenomics and their impact on fungal systematics. Adv Genet. 2017;100:309–328. doi:10.1016/bs.adgen.2017.09.004.

[56] Maharachchikumbura SS, Chen Y, Ariyawansa HA, et al. Integrative approaches for species delimitation in Ascomycota. Fungal Divers. 2021;109(1):155–179. doi:10.1007/s13225-021-00486-6.